

AFRL-AFOSR-UK-TR-2012-0015



Nonlinear Plasmonics in Metamaterials

George P. Tsironis

**Foundation for Research and Technology Hellas (FORTH)
N. Plastira 100, Vassilika Vouton
Heraklion, Greece 70013**

EOARD Grant 10-3039

Report Date: May 2012

Final Report for 05 May 2010 to 04 May 2012

Distribution Statement A: Approved for public release distribution is unlimited.

**Air Force Research Laboratory
Air Force Office of Scientific Research
European Office of Aerospace Research and Development
Unit 4515 Box 14, APO AE 09421**

REPORT DOCUMENTATION PAGE			Form Approved OMB No. 0704-0188		
Public reporting burden for this collection of information is estimated to average 1 hour per response, including the time for reviewing instructions, searching existing data sources, gathering and maintaining the data needed, and completing and reviewing the collection of information. Send comments regarding this burden estimate or any other aspect of this collection of information, including suggestions for reducing the burden, to Department of Defense, Washington Headquarters Services, Directorate for Information Operations and Reports (0704-0188), 1215 Jefferson Davis Highway, Suite 1204, Arlington, VA 22202-4302. Respondents should be aware that notwithstanding any other provision of law, no person shall be subject to any penalty for failing to comply with a collection of information if it does not display a currently valid OMB control number. PLEASE DO NOT RETURN YOUR FORM TO THE ABOVE ADDRESS.					
1. REPORT DATE (DD-MM-YYYY) 30-May-2012		2. REPORT TYPE Final Report		3. DATES COVERED (From – To) 5 May 2010 – 4 May 2012	
4. TITLE AND SUBTITLE Nonlinear Plasmonics in Metamaterials			5a. CONTRACT NUMBER FA8655-10-1-3039		
			5b. GRANT NUMBER Grant 10-3039		
			5c. PROGRAM ELEMENT NUMBER 61102F		
6. AUTHOR(S) Professor George P. Tsironis			5d. PROJECT NUMBER		
			5d. TASK NUMBER		
			5e. WORK UNIT NUMBER		
7. PERFORMING ORGANIZATION NAME(S) AND ADDRESS(ES) Foundation for Research and Technology Hellas (FORTH) N. Plastira 100, Vassilika Vouton Heraklion, Greece 70013			8. PERFORMING ORGANIZATION REPORT NUMBER N/A		
9. SPONSORING/MONITORING AGENCY NAME(S) AND ADDRESS(ES) EOARD Unit 4515 BOX 14 APO AE 09421			10. SPONSOR/MONITOR'S ACRONYM(S) AFRL/AFOSR/RSW (EOARD)		
			11. SPONSOR/MONITOR'S REPORT NUMBER(S) AFRL-AFOSR-UK-TR-2012-0015		
12. DISTRIBUTION/AVAILABILITY STATEMENT Approved for public release; distribution is unlimited. (approval given by local Public Affairs Office)					
13. SUPPLEMENTARY NOTES					
14. ABSTRACT The target of the work is to use Transformation Optics (TO) in order to guide as well as focus plasmons. In the initial phase of the work we focused on using TO to GRaded INdex (GRIN) Lenses of Luneburg type and explored focusing and guiding. In particular we showed both analytically and numerically with home-made codes that for plane wave initial conditions (a) A sequence of Luneburg lenses can form a waveguide with low losses that can guide EM waves in linear as well as curved geometries; (b) Random distributions of Luneburg lenses can lead to the formation of caustics and optical rogue waves; and (c) We used commercial code COMSOL and generated plasmon waves at a metal-dielectric interface. Subsequently we analyzed propagation of Gaussian beams and found that Luneburg lens focusing is not as good as in the case of plane waves. In this case, the addition of nonlinearity of the Kerr type improves focusing and thus propagation in the Luneburg waveguides. In the case of plasmon propagation we found that Luneburg lenses may focus plasmons in a resonant fashion. The results of the Luneburg work formed a manuscript that has been invited to a special volume to be published in the Journal of Optics. This article is currently under review. We anticipate the preparation of one more article with the nonlinear effects.					
15. SUBJECT TERMS EOARD, Plasmons, Plasmonics, Terahertz Emission					
16. SECURITY CLASSIFICATION OF:			17. LIMITATION OF ABSTRACT SAR	18. NUMBER OF PAGES 21	19a. NAME OF RESPONSIBLE PERSON A. TOM GAVRIELIDES
a. REPORT UNCLAS	b. ABSTRACT UNCLAS	c. THIS PAGE UNCLAS			19b. TELEPHONE NUMBER (Include area code) +44 (0)1895 616205

Nonlinear plasmonics in metamaterials
FA8655-10-1-3039 Final report

G. P. Tsironis
(Dated: May 2012)

Summary of results

The target of the work is to use Transformation Optics (TO) in order to guide as well as focus plasmons. In the initial phase of the work we focused on using TO to GRaded INdex (GRIN) Lenses of Luneburg type and explored focusing and guiding. In particular we showed both analytically and numerically with home-made codes that for plane wave initial conditions (a) A sequence of Luneburg lenses can form a waveguide with low losses that can guide EM waves in linear as well as curved geometries. (b) Random distributions of Luneburg lenses can lead to the formation of caustics and optical rogue waves. (c) We used commercial code COMSOL and generated plasmon waves at a metal-dielectric interface. Subsequently we analysed propagation of Gaussian beams and found that Luneburg lens focusing is not as good as in the case of plane waves. In this case, the addition of nonlinearity of the Kerr type improves focusing and thus propagation in the Luneburg waveguides. In the case of plasmon propagation we found that Luneburg lenses may focus plasmons in a resonant fashion.

The results of the Luneburg work formed a manuscript that has been invited to a special volume to be published in the Journal of Optics. This article is currently under review. We anticipate the preparation of one more article with the nonlinear effects.

I. INTRODUCTION

Gradient Index (GRIN) metamaterials are formed through spatial variation of the index of refraction and lead to enhanced light manipulation in a variety of circumstances. These metamaterials provide natural means for constructing various types of waveguides and other optical configurations that guide and focus light in specific desired paths. Different configurations have been tested experimentally while the typical theoretical approach uses Transformation Optics (TO) methods to cast the original inhomogeneous index problem to an equivalent one in a deformed space [2][3][4][5][6]. While this approach is mathematically elegant, it occasionally hides the intuition obtained through more direct means. Furthermore, a general, continuous GRIN waveguide may be hard to analyse in more elemental units and relate its global features to these units. In the present work, we adopt precisely this latter avenue, viz. attempt to construct waveguide structures that are seen as lattices, or networks, of units with specific features. This is a "metamaterials approach", where specific properties of the "atomistic" units are inherited as well as expanded in the network.

The "atomic" unit of the network is a Luneburg lens (LL); the later is a spherical construction where the index of refraction varies from one, in its outer boundary, to $\sqrt{2}$ in the centre with a specific functional dependence on the lens radius [7]. Its basic property, in the geometrical optics limit, is to focus parallel rays on the spherical surface on the opposite side of the lens [7][8][9][10]. This feature makes LL's quite interesting for applications since the focal surface is predefined for parallel rays of any initial angle. While the rays traverse the lens, they suffer variable deflections depending on their distance from the optical axis ray, leading to a point image on the lens surface. This property of the spherical LL is also shared by its cylindrical equivalent formed by long dielectric cylinders while the light wavevector impinges perpendicularly to the cylindrical axis. This geometry turns the problem into a two dimensional one, constructed for any plane that cuts the LL cylinder perpendicular to its axis. The work in this article focuses on exactly this type of cylindrical LLs and, as a result, our approach is strictly two dimensional [7][8][10].

II. SINGLE LUNEBURG LENS

A. Ray tracing solution

The radial dependence of the refractive index n of a planar LL is given by [7]

$$n(r) = \sqrt{2 - \left(\frac{r}{R}\right)^2} \quad (1)$$

where R is the radius of lens while r is the radial distance from the center in the interior of the lens. In order to find an analytical solution for the ray path inside a LL we use Fermat's principle for optical path minimization of the action \mathcal{S} and find [1]

$$r(\phi) = \frac{\mathcal{C}'R}{\sqrt{1 - \sqrt{1 - \mathcal{C}'^2} \sin(2(\phi + \beta))}} \quad (2)$$

where \mathcal{C}' and β are constants. Using appropriate boundary solutions we may obtain analytically the ray propagation in a single Luneburg lens. In Fig. 1 we plot several rays through the analytical solution; it is clear that the solution describes fully the physics of the rays inside a single LL.

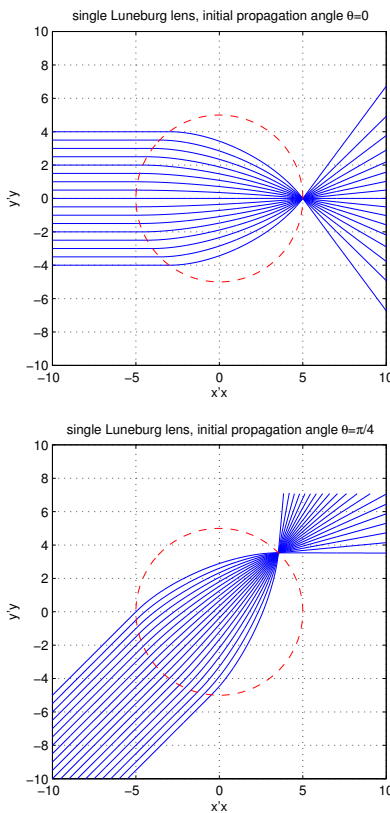


FIG. 1: A Luneburg lens is shown with the red dashed line. The blue lines depict parallel rays for initial propagation angles (i) $\theta = 0$ (upper figure) and (ii) $\theta = \pi/4$ (lower figure). All rays are focused onto a single point on the opposite side of the Luneburg lens leading to thus we have perfect imaging.

III. LUNEBURG LENS WAVEGUIDES

The analytical solution for the ray propagation through a single LL may be used in order to study analytically the ray transfer through various configurations of LLs that form waveguides. Using the initial entry point on the LL (x_0, y_0) as well as the initial ray angle θ the exit point (x, y) and the associated exit angle θ' . We may thus form a mapping from (x_0, y_0, θ) to (x, y, θ') ; further propagation in the surrounding medium is rectilinear while the entry to the next LL is governed by a new initial entry point with angle equal to the previous exit angle. The resulting ray may be traced quite easily.

The first arrangement we use a series of touching LLs on a straight line as in Fig. 2; we note that due to time reversal symmetry the focusing point of a LL produces a ray bunch that exits mutually parallel from the next one. As a result we have the formation of a waveguide, that, depending on whether the number of lenses is even or odd, defocusses or focusses respectively.

The analytical solution may be used for curvilinear arrangements of LLs as well. In Fig. 3 we show a network of 21 Luneburg lenses that are placed in such a way so that to bend light almost at right angle. While there are some ray losses in the bend, the vast majority of the rays pass through leading to an efficient curved waveguide. Choosing an odd total number of lenses leads to focussing in the last lens, while an even number of LLs would give rise to defocussing, as in the linear case.

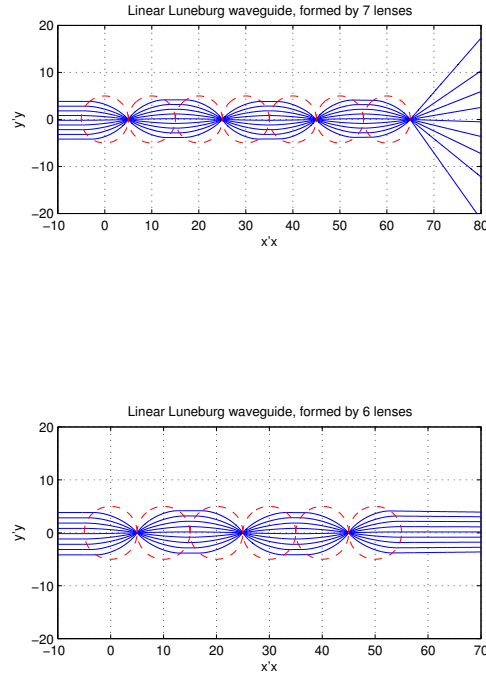


FIG. 2: The red dotted lines denote the arrangement of lenses. The blue lines show the ray tracing. Light is guided by Luneburg lenses across the linear network. (i) Arrangement with 7 lenses (upper figure). We can see that all rays are focus on the last lens. (ii) Arrangement with 6 lenses (lower figure). All rays exit in the same mode as originally entered, i.e. parallel to the waveguid axis.

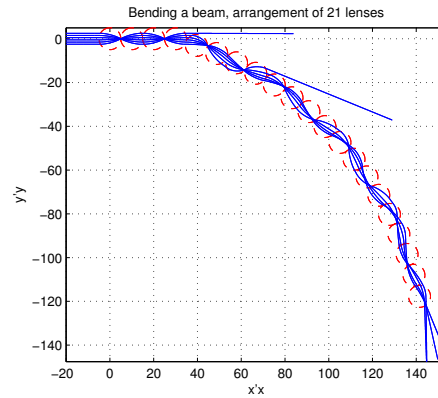


FIG. 3: The red dotted lines denote the network of Luneburg lenses, while the blue lines show the rays. Except for some rays that escape from the waveguide, the majority of rays is guided through the arrangement and exit at right angles wrt the original direction. The rays are focused in the last lens showing the also in curved geometries waveguides with odd number of lenses focus the rays while waveguides with even numbers of LLs do not.

IV. PARAMETRIC RAY SOLUTION FOR SINGLE LUNEBUG LENS

The approach we used [1] is based on an equation that is not a real dynamical equation for a two dimensional (2D) problem, since we have chosen as generalized time one of the space coordinates; i.e. the radial variable r . The

advantage of this choice is that it leads to a one dimensional Lagrangian, that results in equation of motion much easier than if we had a true 2D Lagrangian [1]. Unfortunately, the solution of this equation being a function of ordinate as a function of abscissa fails to work when, for a particular ray or LL arrangement, the ray must bent backwards. The solution to this problem is to find a true 2D equation of motion by using generalized time in addition to the two space coordinates; the Lagrangian in this case contains two spatial coordinates. Unfortunately, the resulting equations are quite complex and we thus use numerics for their direct solution. It is preferable to use Hamilton's equations in Cartesian coordinates; the latter are first order and thus easier to handle numerically. the specific expressions can be found in ref. [1]; we show here the associated figure for a single Luneburg lens.

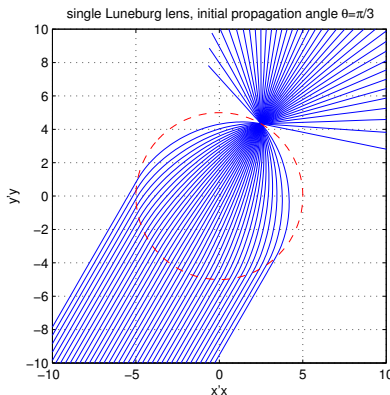


FIG. 4: Use of the Hamiltonian ray-tracing method and through numerical solution of the associated differential equations we obtain the propagation of light through a single Luneburg lens with initial propagation angle $\theta = \pi/5$.

V. WAVE PROPAGATION IN LUNEBURG LENS NETWORKS

We may compare the analytical ray propagation results to simulations that solve directly Maxwell equations. We use the finite difference in time domain (FDTD) method based on Yee's algorithm developed by Allen Taflove [13]. Specifically, FDTD handles light as an electromagnetic field since it solves numerically the fully time dependent Maxwell field equations:

$$\frac{\partial \vec{E}}{\partial t} = \frac{1}{\epsilon} \vec{\nabla} \times \vec{H} \quad (3)$$

$$\frac{\partial \vec{H}}{\partial t} = -\frac{1}{\mu} \vec{\nabla} \times \vec{E} \quad (4)$$

where \vec{E} and \vec{H} denote the electric and magnetic fields respectively, while ϵ and μ are the dielectric permittivity and the magnetic permeability of the medium. Specifically, we consider that the material outside of the LL lens is air, thus setting $\epsilon = \epsilon_0$ and $\mu = \mu_0$, where we have normalized $\epsilon_0 = \mu_0 = 1$. Additionally, inside the lens the permeability is maintained the same, since we consider that the lenses are fabricated by optical materials. On the other hand dielectric permittivity is a function of the position and we can obtain it from the square of the Luneburg refractive index, viz. Eqn. (1), thus

$$\epsilon = n^2 \equiv 2 - \frac{r^2}{R^2} \equiv 2 - \frac{x^2 + y^2}{R^2} \quad (5)$$

We consider TM modes propagating in the x' axis, i.e.

$$E_z = E_y = H_x = 0 \quad (6)$$

As a result, according the condition of the Eq. (6), the Eqns. (3) and (4) take the following form

$$\frac{\partial H_y}{\partial t} = -\frac{1}{\mu} \frac{\partial E_x}{\partial z} \quad (7)$$

$$\frac{\partial H_z}{\partial t} = \frac{1}{\mu} \frac{\partial E_x}{\partial y} \quad (8)$$

$$\frac{\partial E_x}{\partial t} = \frac{1}{\varepsilon} \left(\frac{\partial H_z}{\partial y} - \frac{\partial H_y}{\partial z} \right) \quad (9)$$

Furthermore we use a source creating plane waves [13]. The source is located in the front of the lattice, i.e.

$$E(1, j) = E_0 \sin(\omega t) \quad (10)$$

where the index (1,j) denotes that the source is located on the first section of the lattice in the y-direction, ω is the angular frequency of the EM wave and it is defined as $\omega = 2\pi c/\lambda$, while E_0 is the amplitude of the wave.

In the lattice edge we apply absorbing boundary conditions (ABCs) [13], while we perform all computations in the microwave regime. Specifically, we take the wavelength of the EM wave as $\lambda = 1\text{cm}$. Finally, the radius of each lens in the following simulations, is six times greater than the wavelength, thus $R = 6\lambda = 6\text{cm}$.

In Figs. (5-8) we show the results for the full propagation of EM waves through LLs and LLWs. For each figure, in the upper diagram we plot the steady state of the intensity of the electric field, while in the lower diagram we plot the electric field for a specific time, i.e. we take a snapshot of the electric field. In order to reach steady state of the intensity, we integrate the square of the electric field for one period. Additionally, in order to be sure that the integration is made after the EM wave has passed through the Luneburg network, we choose to average after long time, i.e.

$$I = \lim_{t \rightarrow \infty} \int_t^{t+2\pi} E(r, t)^2 dt \quad (11)$$

In Fig. (5) we show the results for a single LL where we observe focussing on the lens surface in agreement with both the theoretical prediction of Fig. (1) and with Hamiltonian ray tracing method of Fig. (4).

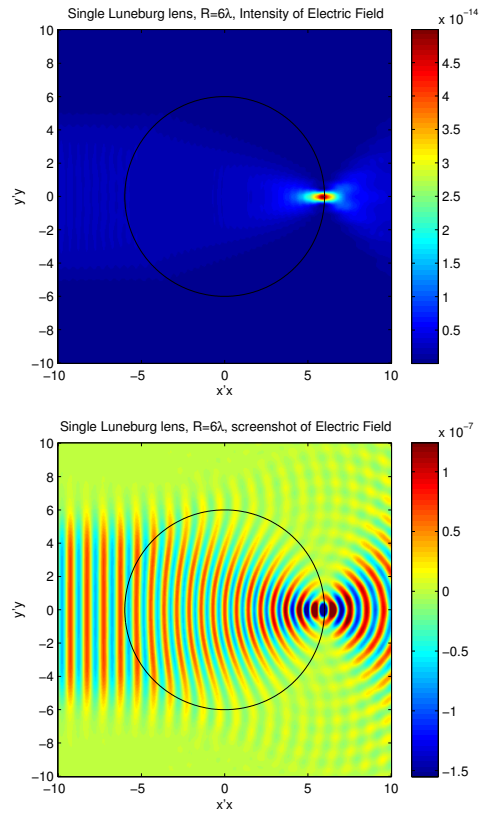


FIG. 5: Simulation with FDTD method for a single Luneburg lens. The EM wave is focused on the surface of the lens. (i) (Upper figure) Plot of the steady state of the intensity I of the electric field. (ii) (Lower figure) Plot of the electric field for a specific time, i.e. a snapshot of the electric field E .

Subsequently we investigate the linear arrangement of LL waveguides with six and seven lenses respectively (Figs. (2) and (5)). In case with even number of lenses, as in Fig. (6), the ray beam is guided and it defocuses in the last lens. On the other hand, in the case with odd number of lenses, as in Fig. (7), the beam is focused on the last lens.

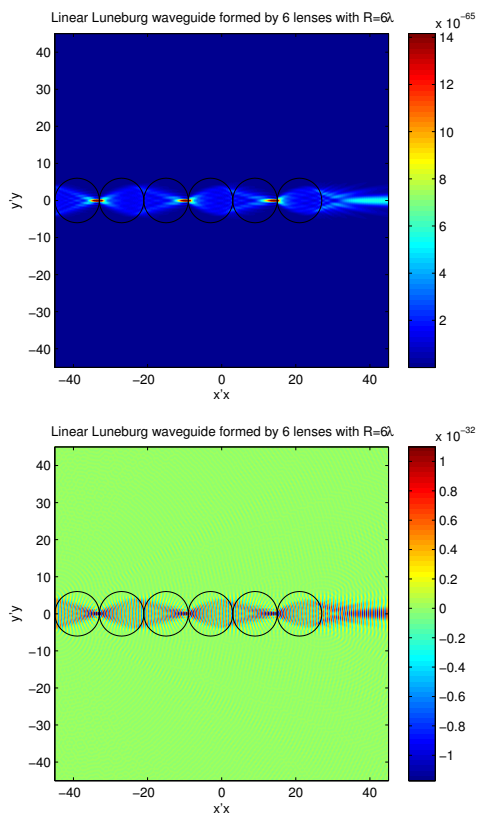


FIG. 6: Simulation with FDTD method. Linear waveguide arrangement formed with six Luneburg lenses. The EM wave is guided through the linear network of lenses and the wave defocuses in the last lens. This result is in agreement with figure 2. (i) (Upper figure) Plot the steady state of the intensity I of the electric field. (ii) (Lower figure) Plot the electric field for a specific time, i.e. a snapshot of the electric field E .

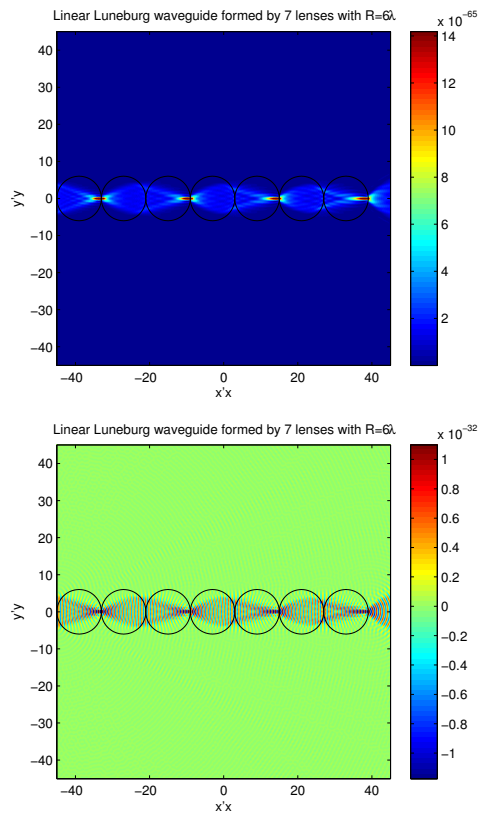


FIG. 7: Simulation with FDTD method. Linear Luneburg waveguide arrangement with seven lenses. Beam guiding and focusing on the surface of the last lens is observed. The result is in agreement figure 2. (i) (Upper figure) Plot the steady state of the intensity I of the electric field. (ii) (Lower figure) Plot the electric field for a specific time, i.e. a snapshot of the electric field E .

In the Fig. (8) we investigate right angle light bending while in Fig. (9) we have a circular arrangement of LL's. We observe propagation and guiding with small losses.

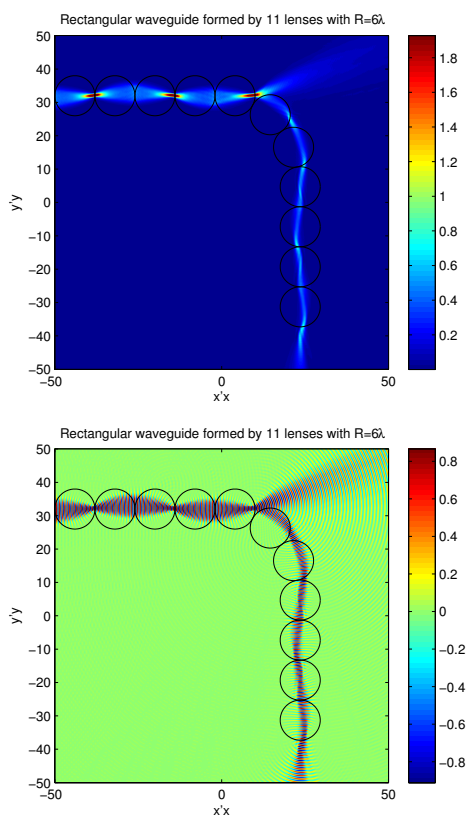


FIG. 8: A rectangular waveguide is formed with eleven Luneburg lenses. The EM wave is guided and bends at right angles through a network of lenses. (i) (Upper figure) Plot the steady state of the intensity I of the electric field. (ii) (Lower figure) Plot the electric field for a specific time, i.e. a snapshot of the electric field E .

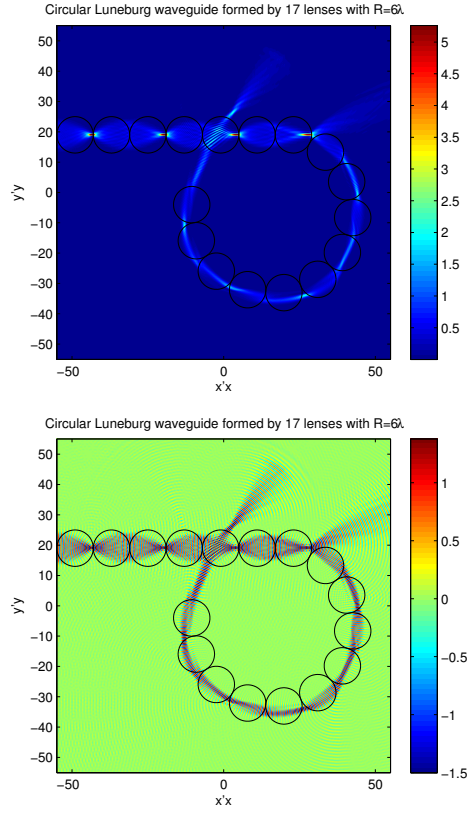


FIG. 9: A circular waveguide formed by seventeen Luneburg lenses. The EM wave is guided through a circular orbit. (i) (Upper figure) Plot the steady state of the intensity I of the electric field. (ii) (Lower figure) Plot the electric field for a specific time, i.e. a snapshot of the electric field E .

VI. LUNEBURG NONLINEAR EFFECTS

In order to analyze specific, realistic geometries we purchased and implemented in the context of the present grant the commercial package COMSOL. During the initial learning phase we studied simple dielectric structures. Subsequently we entered the study of specific LL configurations as well as investigated the role of nonlinearity in GRIN media made of Luneburg lenses. While plane waves focus perfectly in LLs, more realistic wavepackets have distortions. Specifically, we tested initially gaussian as well as square wave sources and found that LL focusing takes place slightly outside the lens. This distortion can be corrected through nonlinearity. The results are shown in Fig. 10.

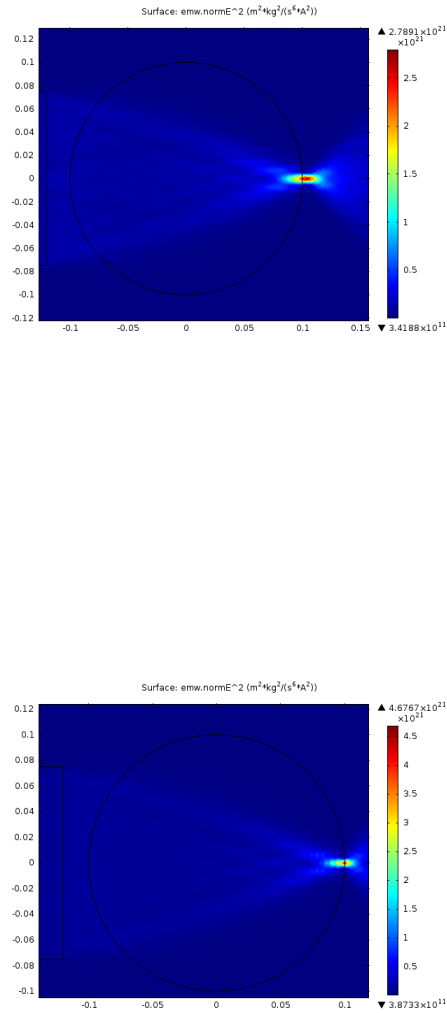


FIG. 10: (a) Square wave-single frequency pulse focusing in a single Luneburg lens, (b) Same as in (a) but with nonlinearity $\chi = 1.0 \times 10^{-22}$. We observe improvement in focusing induced through nonlinearity

We may also form similarly an LL waveguide and observe the improvement in focusing and propagation as in Fig.

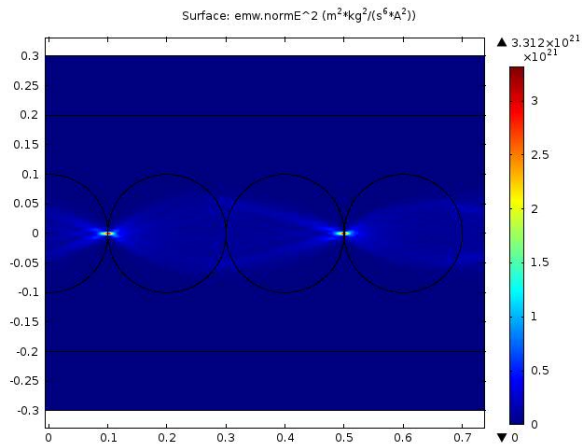
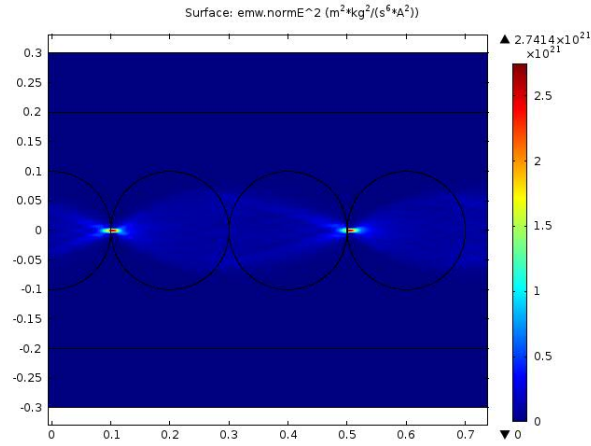


FIG. 11: (a) Square wave-single frequency pulse propagation in a linear four Luneburg lens waveguide, (b) Same as in (a) but with nonlinearity $\chi = 1,0 \times 10^{-22} m^2/V^2$. We observe improvement in focusing and propagation induced through nonlinearity

Distribution A: Approved for public release; distribution is unlimited.

VII. LUNEBURG PLASMON FOCUSING

Finally, we used the commercial package COMSOL in order to study the effect of LL focusing of plasmons. The results show that evanescent field focusing results in plasmon wave concentration. The geometry we use involves two half planes, the lower one being a metal (gold) while the upper one a dielectric (air). In the upper plane we place (half) Luneburg lenses. What we are interested in is the focusing and manipulation of plasmons generated on the interface through LLs. In Fig (12) we show wave focusing in the dielectric that results in focusing of the surface plasmon that is generated at the interface. IN Fig (13) we have an array of seven lenses in the dielectric plane. The impinging microwave radiation generates surface plasmons that propagate across the interface together with the wave in the dielectric part that is being focused by the LL's. IN Fig. (14) we show the wave amplitude just above and just below the interface across the propagation direction. We observe the focusing effect of the Luneburg lenses (a) while, at the same time, we see a resonant enhancement of the plasmon wave in the metal. This is a very interesting effect that we believe stems from the matching of the propagating surface plasmon to the focusing of the wave in the dielectric by the Luneburg lenses. We are currently studying this peculiar effect analytically and we believe that shortly we will be able to address it quantitatively. It is obvious that this effect is potentially very interesting for plasmon decay suppression during propagation.

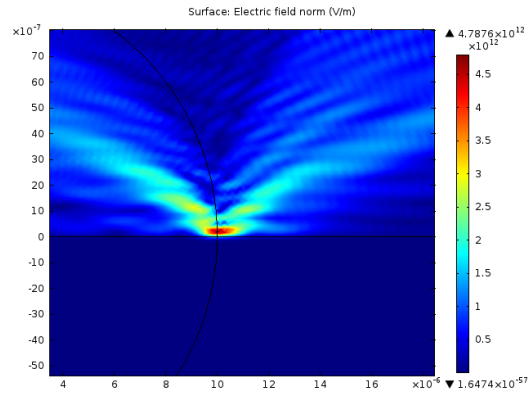
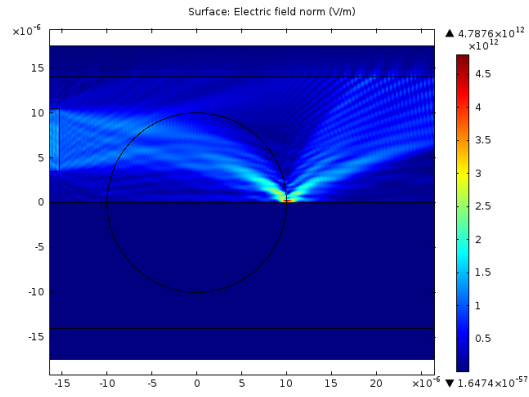


FIG. 12: (a) Square wave-single frequency pulse propagation in a single Luneburg lens in touch with a metal (gold). We observe plasmon focusing. (b) Zoom of (a) in the focusing region

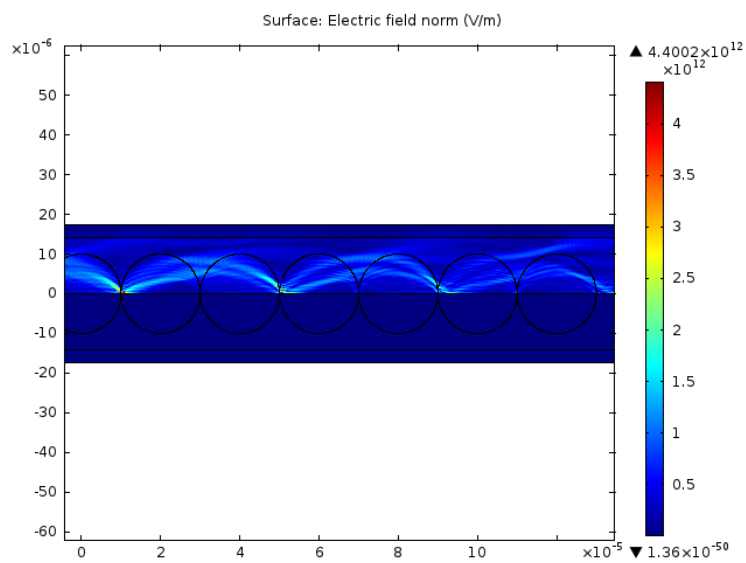


FIG. 13: Generation, propagation and focusing of plasmons in a Luneburg lens waveguide.

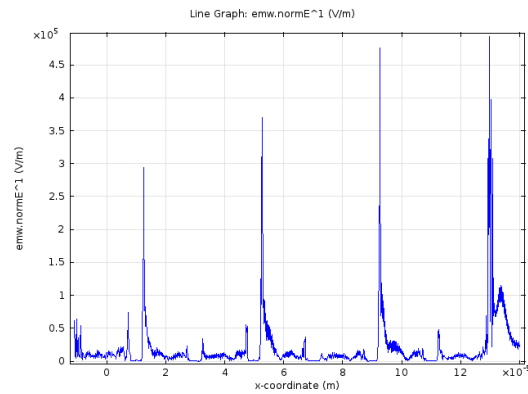
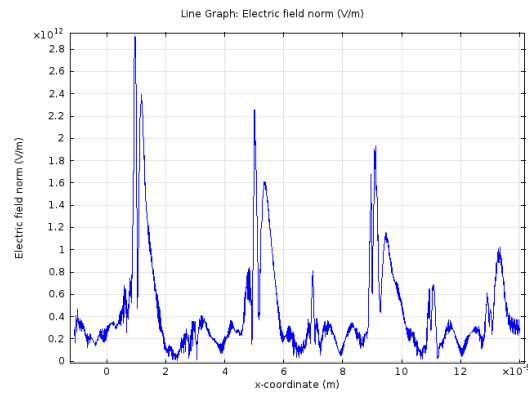


FIG. 14: (a) Electric field distribution along the propagation direction of Fig. (13) in the dielectric just above the interface. We observe the Luneburg induced focusing. (b) Electric field plasmon distribution just below the interface. We observe plasmon resonant enhancement.

-
- [1] M. Mattheakis, G. P. Tsironis and V. I. Kovanis, Luneburg lens waveguide networks, submitted to the Journal of Optics.
 - [2] A.V. Kildishev, V.M Shalaev, *Transformation optics and metamaterials*, Physics-Uspokhi **54** 53-63 (2011).
 - [3] H.Chen, C.T.Chan, P.Sheng, *Transformation optics and metamaterials*, Nature Materials **9**, 387-396 (2010)
 - [4] D.Schurig, J.B. Pendry, D.R.Smith, *Calculation of material properties and ray tracing in transformation media*, OPTICS EXPRESS **14** 21 (2006)
 - [5] J.B.Pendry, D.Schurig, D.R.Smith, *Controlling Electromagnetic Fields*, Science Express 10.1126 (2006)
 - [6] U.Leonhardt, T.Philbin, *Transformation Optics and the Geometry of Light* Prog. Opt **53**, 69-152 (2009)
 - [7] R.K.Luneburg, *Mathematical Theory of Optics*, University of California press, Berkeley and Los Angeles (1964).
 - [8] S.P. Morgan, *General Solution of the Luneburg Problem*, journal of applied physics **29** 9, 1358-1368 (1958).
 - [9] A.Falco, S.C. Kehr, and U. Leonhardt, *Luneburg lens in silicon photonics*, OPTICS EXPRESS **19** 6 (2011).
 - [10] J.Sochacki, *Exact analytical solution of the generalized Luneburg lens problem*, JOSA A **73** 6 (1982)
 - [11] V.Lakshminarayanan A.K.Ghatak K.Tyagaraajan, *Lagrangian Optics*, Kluwer Academic Publishers, Springer (2002).
 - [12] O. N. Stavroudis, *The Mathematics of Geometrical and Physical Optics: The k-function and its Ramifications* Willey-VCH, Weinheim (2006)
 - [13] A.Taflove S.C.Hagness, *Computational Electrodynamics: The Finite-Difference Time-Domain method*, Artech House Norwood MA 02062 (2005).
 - [14] P.Stellman K.Tian G.Barbastathis, *Design of Gradient Index (GRIN) Lens Using Photonic Non-Crystals*, in Conference on Lasers and Electro-Optics/Quantum Electronics and Laser Science Conference and Photonic Applications Systems Technologies, OSA Technical Digest (CD) (Optical Society of America, 2007), paper JThD121.
 - [15] S. Takahashi, C. Chang, S. Yang, H. J. Choi, G. Barbastathis, *Fabrication of Dielectric Aperiodic Nanostructured Luneburg Lens in Optical Frequencies*, in Quantum Electronics and Laser Science Conference, OSA Technical Digest (CD) (Optical Society of America, 2011), paper QTuM2.
 - [16] H.Gao, S.Takahashi, L.Tian, G.Barbastathis, *Aperiodic subwavelength Luneburg lens with nonlinear Kerr effect compensation*, OPTICS EXPRESS **19** 3 (2011).
 - [17] N.A. Mortensen, O. Sigmund, O. Breinbjerg, *Prospects for poor-man's cloaking with low-contrast all-dielectric optical elements*, Journal of the European Optical Society-Rapid Publication **4** 09008 (2009).
 - [18] T.Zentgraf, Y.Liu, M.H.Mikkelsen, J.Valentine, X.Zhang, *Plasmonic Luneburg and Eaton lenses*, Nature Nanotechnology **6** 3, 151-155 (2011)
 - [19] Ulf Leonhardt, *Notes on conformal invisibility devices*, New Journal of Physics **8** 118 (2006)